Notes

Gas Permeability and Phase Morphology of Poly(1-(trimethylsilyl)-1-propyne)/ Poly(1-phenyl-1-propyne) Blends

Lora G. Toy,[†] Benny D. Freeman,*[,†] and Richard J. Spontak[‡]

Departments of Chemical Engineering and Materials Science and Engineering, North Carolina State University, Raleigh, North Carolina 27695

Atsushi Morisato and Ingo Pinnau*

Membrane Technology and Research, Inc., 1360 Willow Road, Suite 103, Menlo Park, California 94025

Received January 22, 1997
Revised Manuscript Received May 19, 1997

Physical blends and copolymers of poly(1-(trimethylsilyl)-1-propyne) (PTMSP) and poly(1-phenyl-1-propyne) (PPP) have recently been the focus of several gas transport studies.[1−5] Both materials are glassy, disubstituted polyacetylenes but have very different permeation characteristics. Being the most gas-permeable polymer known,[6] PTMSP has an extremely high fractional free volume and possesses unusual vapor transport properties. It is more permeable to large, condensable vapors (e.g., *n*-butane) than to small, noncondensable gases (e.g., hydrogen).[4,7] In fact, PTMSP exhibits very high selectivity for vapors and high vapor permeability for mixtures containing noncondensable gases.[5,7,8] This vapor-selective behavior is atypical of the gas-selective nature of conventional, low-free-volume glasses and is attributed to the exceptionally high free volume in PTMSP. In contrast, PPP, which has a substantially lower free volume than PTMSP, displays transport characteristics of conventional glassy polymers; that is, PPP is gas-selective, exhibiting higher permeabilities for small gases than for large vapors.[4]

The combination of high mixture vapor permeability and selectivity makes PTMSP an ideal polymeric membrane material for industrial vapor separations. However, gas transport properties of PTMSP are notoriously unstable. Its high permeabilities decrease dramatically with time due to physical aging, sorption of condensable contaminants from the environment, and chemical aging.[9,10] Gas permeabilities of PPP, unlike those of PTMSP, are relatively stable with time.[2] To control the permeability deterioration of PTMSP, a multicomponent system approach has focused on blending or copolymerizing PTMSP with small quantities (<10 wt %) of PPP to stabilize PTMSP gas transport properties against physical aging.[1,2] Because PPP gas permeability is at least 2 orders of magnitude lower than that of PTMSP, a high PPP content in these bicomponent systems would impair the inherently high gas permeability of PTMSP. Previous investigations[1−5] have, therefore, focused on blend and copolymer systems with low PPP concentration to evaluate the utility of these systems as potential membrane materials for gas and vapor separation applications. In this work, gas permeation characteristics of PTMSP/PPP blends, varying in composition from 0 to 100 wt % PTMSP, are discussed in terms of blend morphology observed using transmission electron microscopy (TEM).

The PTMSP was kindly supplied by Air Products and Chemicals, Inc. (Allentown, PA) and Permea, Inc. (St. Louis, MO) and used as-received, whereas the PPP was synthesized according to the protocol described earlier.[4] Blend films for gas permeation analysis were prepared by dissolving predetermined quantities of PTMSP and PPP in toluene to form 2 wt % solutions. To control film thickness, a doctor blade was used to cast these solutions onto a glass plate. Blend samples for TEM analysis were cast from 1.7 wt % toluene solutions into flat-bottomed Teflon molds. All films were dried slowly at ambient conditions for 24 h (permeation) to 3 weeks (TEM) and then placed in a vacuum oven held at 80−90 °C for 3 days to remove residual solvent. Resultant films measured 20−30 μm thick for permeation testing and about 300 μm thick for TEM specimen preparation and were sufficiently strong (mechanically) at all compositions to permit easy handling. Pure nitrogen and carbon dioxide permeabilities of PTMSP/PPP blend membranes were determined with an error of ±5% at 25 °C using the constant pressure/variable volume method.[11] The feed pressure used in these experiments was 4.5 atm, while the permeate pressure was maintained at 1 atm. Corresponding films for TEM were sectioned in a Reichert-Jung Ultracut-S cryoultramicrotome at −100 °C. Electron-transparent sections were imaged without staining on a Zeiss EM902 electron spectroscopic microscope operated at 80 kV and an energy loss (ΔE) of 20−100 eV.

The gas permeation behavior of PTMSP/PPP blends as a function of composition is presented in Figure 1a,b. As the PPP content increases, the carbon dioxide and nitrogen permeabilities decrease substantially, whereas the carbon dioxide/nitrogen selectivity increases dramatically. Moreover, as shown clearly in Figure 1b, the permeability and selectivity exhibit a sigmoidal dependence on composition and start to change markedly at low PPP concentrations (∼3−20 wt %). The trends evident in Figure 1 are consistent with those reported[4] earlier for oxygen and *n*-butane in similar blends and permit a qualitative assessment of blend morphology since the permeating gas molecules serve as microstructural probes. A sigmoidal dependence of permeability and selectivity on blend composition is characteristic of immiscible (phase-separated) polymer blend systems in which bulk properties are dominated by the continuous phase.[12,13] Over a relatively small composition range, these biphasic blends undergo a transition from one phase being continuous and property-controlling to the other phase assuming these roles.[12,13] Such "phase inversion" is responsible for the S-shaped (sigmoidal) nature of the permeability and selectivity vs composition curves generated from immiscible polymer blends. Figure 1 suggests, therefore, that PTMSP/PPP blends

* To whom correspondence should be addressed.
[†] Department of Chemical Engineering.
[‡] Department of Materials Science and Engineering.

S0024-9297(97)00091-0 CCC: $14.00

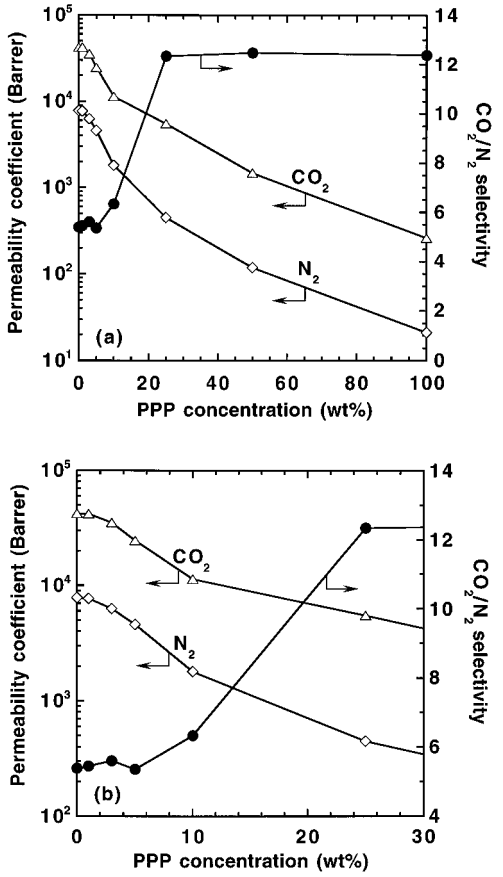

Figure 1. Effect of blend composition on CO_2 (△) and N_2 (◇) permeabilities and CO_2/N_2 selectivity (●) for PTMSP/PPP blends at 25 °C: (a) 0−100 wt % PPP (entire PPP composition range); (b) 0−30 wt % PPP (low PPP composition range). The feed and permeate pressures are 4.5 and 1 atm, respectively. [Note: 1 Barrer = 10^{-10} (cm^3(STP)·cm)/(cm^2·s·cmHg).]

are phase-separated, which is corroborated by earlier solid-state NMR studies of this system.[4] Below 3 wt % PPP, PTMSP is the continuous phase governing the gas transport properties since the measured blend permeabilities and selectivities are nearly identical to those of pure PTMSP. For PPP concentrations above 20 wt %, PPP constitutes the mass-transport-controlling phase. Between 3 and 20 wt % PPP, the selectivity increases abruptly from values similar to those of PTMSP to values resembling those of PPP, while the permeability decreases most strongly over this composition range. This rapid change in permeability and selectivity over a very narrow, PTMSP-rich composition range suggests that these properties are highly sensitive to the degree of connectivity or overlap of the PPP domains in the blend.

Permeability data for the phase-separated blends may be compared to predictions of the generalized Maxwell model for gas transport in heterogeneous media. This model describes the compositional dependence of permeation properties in binary media consisting of microparticulate dispersions of one component in a continuous matrix of a second component and can be expressed as[14]

$$P_{\text{blend}} = P_c\left[1 + \frac{(1+G)\phi_d}{\left(\frac{P_d/P_c + G}{P_d/P_c - 1}\right) - \phi_d}\right] \qquad (1)$$

In eq 1, P_{blend}, P_c, and P_d are the blend, continuous-phase, and dispersed-phase permeabilities, respectively, and ϕ_d is the dispersed-phase volume fraction. Here, G is a geometric factor accounting for the effect of dispersion shape. For spherical (isometric) dispersions, G is 2; for long, cylindrical (elongated) dispersions transverse to the gas flow direction, G equals 1.[14] In the case of planar (laminate) structures, G is infinity if the laminae are parallel to the flow direction and zero if they are oriented normal to this direction.[14] The laminate structure provides upper and lower bounds for the generalized Maxwell model. The upper bound, corresponding to minimum flow obstruction, is obtained when G is infinity; the lower bound, corresponding to maximum flow obstruction, is obtained for G equal to zero.[14] Model predictions using intermediate G values between zero and infinity lie between these two extremes. Furthermore, at the limiting G values, the model reduces to one that depends only on blend composition, predicting identical blend permeability values irrespective of which phase is presumed to be continuous. In contrast, model predictions at intermediate G values depend on both blend composition and the component assumed to be the continuous phase.

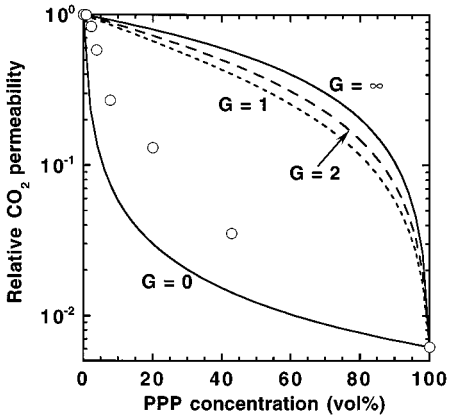

Figure 2. Comparison of CO_2 permeability (○) in PTMSP/PPP blends relative to that in pure PTMSP with theoretical predictions from the generalized Maxwell permeation model for heterogeneous media at various geometric factor (G) values: $G = \infty$ for PPP laminae parallel to the gas flow direction; $G = 2$ for PPP spheres; $G = 1$ for long PPP cylinders transverse to the flow direction; and $G = 0$ for PPP laminae perpendicular to the flow direction. For $G = 2$ and $G = 1$, the model assumes that the PPP phase is dispersed in a continuous PTMSP phase. For the limiting cases of $G = \infty$ and $G = 0$, a defect-free laminate structure of PTMSP and PPP is assumed.

Generalized Maxwell model predictions using various G values are compared to the carbon dioxide permeation data as a function of PPP volume fraction (calculated as described earlier[4]) in Figure 2. Theoretical predictions that assume a dispersion of either PPP spheres ($G = 2$) or long, transverse PPP cylinders ($G = 1$) in a continuous PTMSP matrix agree with the experimental data only at PPP concentrations below 5 wt % (3.8 vol %). At higher PPP compositions, the blend permeability is greatly overestimated by these predictions. Physically, the deviation of the measured permeability values from those of the model with $G = 2$ and $G = 1$ reflects the tendency of PPP domains to overlap and form more effective barriers to gas permeation at higher PPP content. The permeability data, in fact, do approach the laminate structure limit ($G = 0$) in which laminae are oriented perpendicular to the flow direction and the obstruction to gas flow is maximized. However, the actual blend permeability is still higher than the model prediction with $G = 0$, suggesting that PTMSP-

rich blends having more than 5 wt % PPP behave as very defective laminates. A similar analysis of the nitrogen permeation data yields identical results. Generalized Maxwell model predictions, therefore, suggest that PTMSP/PPP blend permeation properties depend strongly on the dispersed-PPP-phase connectivity and approach those of highly defective, layered composites. These predictions are consistent with the blend morphology inferred from the permeation behavior seen in Figure 1.

A series of TEM micrographs for three blend compositions is presented in Figure 3. Relative to the PPP phase, the silicon-rich PTMSP phase appears electron-opaque (dark) in these images. The micrographs in Figure 3 confirm the phase-separated nature of the blends examined and reveal that PPP domains exist as ellipsoidal dispersions in a PTMSP matrix. Measuring between 0.2 and 0.3 μm wide and up to 1.5 μm long, highly elongated PPP dispersions in the 3 wt % PPP blend (Figure 3a) exhibit aspect ratios ranging from 5 to 8. Likewise, PPP dispersions in the 10 wt % PPP blend (Figure 3b) also appear highly elongated. In this case, large domains measure about 0.7−0.9 μm in thickness and up to approximately 5 μm in length. Two features of Figure 3b warrant particular attention. First, the aspect ratios of PPP domains in the 10 wt % PPP blend lie within the same range as those in Figure 3a for the 3 wt % PPP blend. In addition, the existence of numerous, highly elongated PPP domains in Figure 3b suggests that the blend is nearly stratified along the direction normal to the long axis of the domains. When the PPP content is increased to 25 wt %, PPP dispersions remain substantially drawn, measuring on the order of several microns along their thin axis (Figure 3c). Furthermore, the minor PPP phase begins to appear much more inhomogeneously layered due to the extended length of neighboring PPP domains.

In the 3 and 10 wt % PPP blends, the PPP phase exists as discrete, extended dispersions. The number density of PPP domains, however, remains relatively small at 3 wt % PPP, in which case the PTMSP matrix must remain essentially unobstructed, thereby providing a continuous pathway for permeating gas molecules. At 10 wt % PPP, both the size and number density of PPP dispersions increase, and the discrete dispersions start to overlap along the direction normal to their long axis. If this normal direction coincides with that of gas permeation, then the PPP domains will act as local permeation barriers because PPP is significantly less permeable than PTMSP. The blend would effectively behave as a highly defective laminate composed of PTMSP and PPP "layers." Blend permeability would thus be dominated by the less permeable PPP phase.

Under such conditions, permeability decreases because penetrant molecules must travel a more tortuous path around the PPP barriers. As the PPP domains are also somewhat permeable, the more tortuous the route through the PTMSP phase, the more important the influence of the PPP phase on the overall blend permeability and selectivity. With increasing PPP content, the connectivity or overlap of the dispersed PPP phase increases, leading to even greater permeability reduction and selectivity increase. When the PPP dispersions overlap sufficiently to form an effectively defect-free layer in the blend film, the selectivity is essentially that of PPP and becomes independent of PPP concentration. The permeability, however, continues to decrease monotonically with increasing PPP content as the low-permeability PPP phase plays an increasingly greater role in the overall blend permeation behavior. On the other hand, if the gas permeation direction is parallel

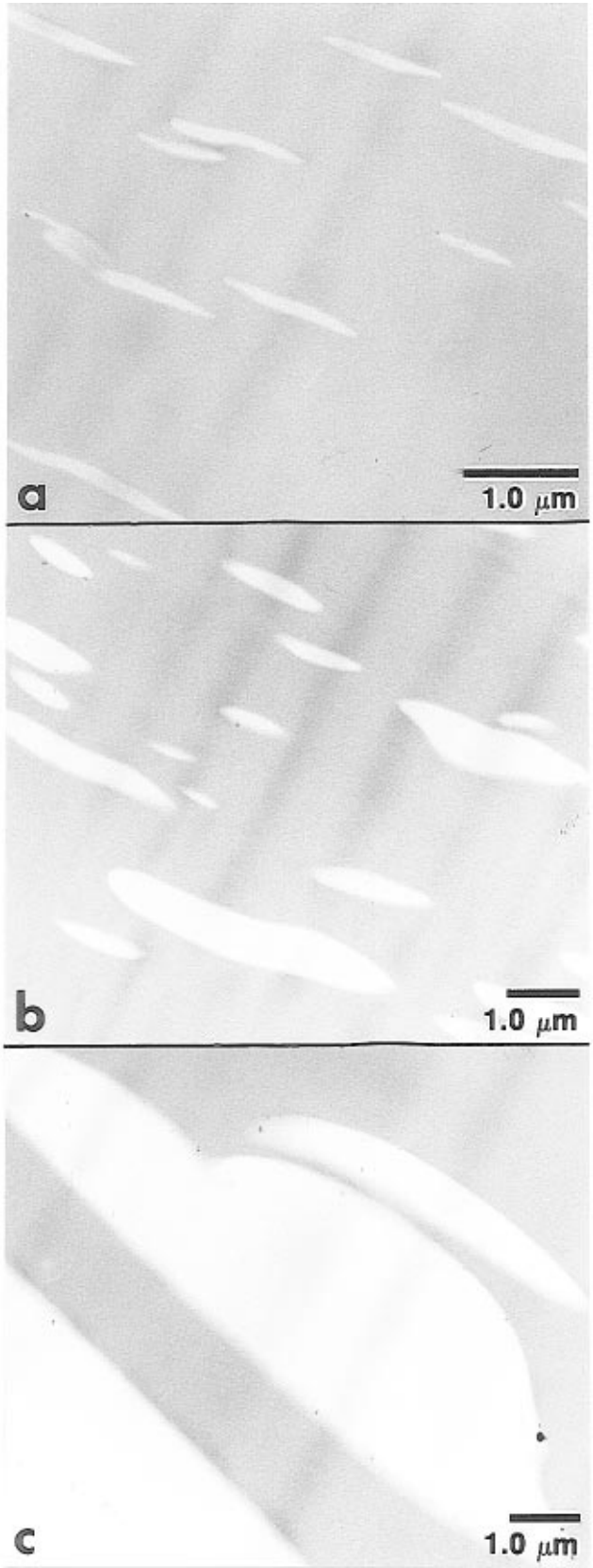

Figure 3. Transmission electron micrographs of PTMSP/PPP blends at three blend compositions (in wt % PPP): (a) 3; (b) 10; (c) 25. Due to differences in electron density, the PTMSP-rich phase is electron-opaque (dark) in these micrographs. Note that the light PPP dispersions appear as highly elongated ellipsoids, increasing in both size and overlap with increasing PPP content.

to the long axis of the PPP domains, then permeating molecules would be virtually unobstructed by PPP ellipsoids in the 3 and 10 wt % PPP blends. Consequently, gas transport should not be greatly affected by the presence of added PPP.

The experimental results in Figures 1 and 2 clearly reveal that the gas transport properties of PTMSP/PPP blends are very sensitive to composition. Permeability decreases markedly when the PPP concentration exceeds 3 wt %, and selectivity more than doubles as the PPP content increases from 10 to 20 wt %. Electron micrographs confirm that these blends are phase-separated and show that the less permeable PPP phase exists as highly extended, ellipsoidal dispersions in a PTMSP matrix. Correlation of gas permeability and blend morphology suggests that the PPP ellipsoids are most probably oriented with their long axis perpendicular to the gas transport direction. The morphological features of PTMSP-rich blends approach that of a highly defective, layered composite (laminate) due to an increase in the overlap of PPP dispersions when the PPP content increases above 3 wt %. This interpretation explains the substantial permeability reduction and selectivity increase observed at low PPP concentrations. This morphology-based permeation model is also consistent with predictions from the generalized Maxwell formalism if PPP provides the dominant resistance to gas transport above 5 wt % PPP.

Acknowledgment. The authors gratefully acknowledge partial support of this work by the Department of Energy through the Small Business Innovation Research Program (Grant Number DE-FG03-94ER81811) and the National Science Foundation [NSF Young Investigator Award CTS-9257911 (B.D.F.)].

References and Notes

(1) Nakagawa, T. *Proceedings of the International Congress on Membranes and Membrane Processes (ICOM)*, Yokohama, Japan, 1996; pp 272−273.
(2) Nagai, K.; Higuchi, A.; Nakagawa, T. *J. Polym. Sci., Part B: Polym. Phys.* **1995**, *33*, 289.
(3) Morisato, A.; Freeman, B. D.; Pinnau, I.; Casillas, C. G. *J. Polym. Sci., Part B: Polym. Phys.* **1996**, *34*, 1925.
(4) Morisato, A.; Shen, H. C.; Sankar, S. S.; Freeman, B. D.; Pinnau, I.; Casillas, C. G. *J. Polym. Sci., Part B: Polym. Phys.* **1996**, *34*, 2209.
(5) Pinnau, I.; Casillas, C. G.; Morisato, A.; Freeman, B. D. *J. Polym. Sci., Part B: Polym. Phys.* **1996**, *34*, 2613.
(6) Masuda, T.; Isobe, E.; Higashimura, T.; Takada, K. *J. Am. Chem. Soc.* **1983**, *105*, 7473.
(7) Pinnau, I.; Toy, L. G. *J. Membr. Sci.* **1996**, *116*, 199.
(8) Srinivasan, R.; Auvil, S. R.; Burban, P. M. *J. Membr. Sci.* **1994**, *86*, 67.
(9) Odani, H.; Masuda, T. In *Polymers for Gas Separation*; Toshima, N., Ed.; VCH: New York, 1992; pp 107−144.
(10) Nagai, K.; Nakagawa, T. *J. Appl. Polym. Sci.* **1994**, *54*, 1651.
(11) Stern, S. A.; Gareis, P. J.; Sinclair, T. F.; Mohr, P. H. *J. Appl. Polym. Sci.* **1963**, *7*, 2035.
(12) Shur, Y. J.; Rånby, B. *J. Appl. Polym. Sci.* **1975**, *19*, 1337.
(13) Hopfenberg, H. B.; Paul, D. R. In *Polymer Blends*; Paul, D. R., Newman, S., Eds.; Academic Press: New York, 1978; Vol. 1; pp 445−489.
(14) Petropoulos, J. H. *J. Polym. Sci., Polym. Phys. Ed.* **1985**, *23*, 1309.

MA970091T